

Available online at: <https://ijact.in>

Date of Submission	23/12/2019
Date of Acceptance	16/03/2020
Date of Publication	31/05/2020
Page numbers	3690-3697 (8 Pages)

**Cite This Paper:** Kuntida K, S.Koonprasert, Akapak C. Three types of kinetics and instability for enzymatic glucose fuel cell models, 9(5), COMPUSOFT, An International Journal of Advanced Computer Technology. PP. 3690-3697.

This work is licensed under Creative Commons Attribution 4.0 International License.



An International Journal of Advanced Computer Technology

ISSN:2320-0790

## THREE TYPES OF KINETICS AND INSTABILITY FOR ENZYMATICAL GLUCOSE FUEL CELL MODELS

Kuntida Kawinwit<sup>1</sup>, Sano Koonprasert<sup>2,4</sup>, Akapak Charoenloedmongkhon<sup>3,4</sup>

<sup>1</sup>Graduate student in Department of Mathematics, Faculty of Applied Science, King Mongkut's University of Technology North Bangkok, Bangkok 10800, Thailand.

<sup>2</sup>Associate Professor in Department of Mathematics, Faculty of Applied Science, King Mongkut's University of Technology North Bangkok, Bangkok 10800, Thailand.

<sup>3</sup>Lecturer in Department of Mathematics, Faculty of Applied Science, King Mongkut's University of Technology North Bangkok, Bangkok 10800, Thailand.

<sup>4</sup>A researcher in Centre of Excellence in Mathematic, CHE, Si Ayutthaya Road, Bangkok, Bangkok 10400, Thailand [kun.kuntitda02@gmail.com](mailto:kun.kuntitda02@gmail.com)<sup>1</sup>, [sano.k@sci.kmutnb.ac.th](mailto:sano.k@sci.kmutnb.ac.th)<sup>2</sup>, [akapak.c@sci.kmutnb.ac.th](mailto:akapak.c@sci.kmutnb.ac.th)<sup>3</sup>

**Abstract:** Mathematical modeling plays an important role in biochemistry having various enzymatic fuel cell problems. Enzymes are the basis of life activities and involved in almost all chemical reactions in organisms. The metabolic system of many anabolic and catabolic reactions under the catalysis of enzymes, which the study of the chemical reactions that are catalyzed by enzymes is called enzyme kinetics. This paper aims to discuss the enzyme kinetics term of the enzymatic glucose fuel cells. We apply three types of enzyme kinetics including the Michaelis Menten equation, the Morrison equation (Quadratic Velocity Equation) and the multiple substrate binding sites into the models. We analyze the equilibrium points, local stability of the models and plot some graphs of the glucose and hydrogen ion concentrations with time across the enzymatic glucose fuel cells by the Maple program.

**Keyword:** Michaelis Menten equation; Morrison equation; Multiple substrate binding sites equation; Partial differential equation

### I. INTRODUCTION

In biological chemistry systems, the enzymatic fuel cells (EFCs) have emerged as an eco-friendly energy-producing technology based on the capacity of naturally available redox enzymes to transform a wide diversity of fuels and oxidants with high specificity and high-efficiency [1]. Glucose is a metabolic intermediate which implicated with many of the body's essential processes when coupled to a reduction reaction; electrochemical glucose oxidation allows generating energy called glucose fuel cells. It enables such energy harvesting via chemical mechanisms from blood metabolites such as glucose, wherein the electrodes modified with naturally occurring glucose and oxygen

selective enzymes derived from micro-organisms are used to oxidize and reduce glucose and oxygen, respectively. Enzyme kinetics is the study of the chemical reactions that are catalyzed by enzymes. It has been around for a long time, as one of the earliest areas where mathematics was utilized to understand biological phenomena. The chemical reaction between enzyme and glucose is shown in Figure 1 illustrated in the following diagram.



Figure 1: Schematic diagram of the chemical reaction between enzyme and glucose.

In Figure 1, the Michaelis Menten equation [5] which is one of the best-known model of enzyme kinetics with the reaction rate are

$$f(C_G) = \frac{V_{max}[C_G]}{K_m + [C_G]}, \quad (1)$$

where  $f(C_G)$  is reaction velocity to glucose concentration,  $C_G$  is concentration of glucose in the enzyme layer,  $V_{max} = K_{cat}[E_T]$  is the maximum velocity achieved by the system at maximum (saturating) glucose concentrations,  $K_m$  is Michaelis Menten constant. On the other hand, Schematic diagram provides the Morrison equation (Quadratic Velocity equation) [6] with the reaction rate as:

$$f(C_G) = V_{max} \frac{(a + [C_G]) - \sqrt{(a + [C_G])^2 - 4[E][C_G]}}{2[E]}, \quad (2)$$

where  $a = [E] + K_m$ ,  $[E]$  is given by  $T[E_T]$  when  $T$  is the thickness of the enzyme layer.

Moreover, the reaction of multiple substrate binding sites [7] can be determined by Schematic diagram in Figure 2. with the reaction rate  $f(C_G)$  as:

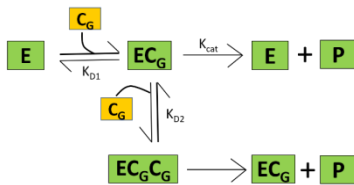
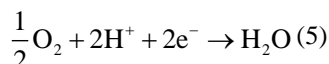


Figure 2: Schematic diagram of the multiple substrate binding sites.

$$f(C_G) = \frac{V_{max1} \frac{[C_G]}{K_{D1}} + V_{max2} \frac{[C_G]^2}{K_{D1}K_{D2}}}{1 + \frac{[C_G]}{K_{D1}} + \frac{[C_G]^2}{K_{D1}K_{D2}}}, \quad (3)$$

where  $V_{max1} = K_{cat1}[E_T]$ ,  $V_{max2} = K_{cat2}[E_T]$ ,  $K_{D1} = \frac{[E][C_G]}{[EC_G]}$ ,  $K_{D2} = \frac{[EC_G][C_G]}{[EC_G C_G]}$ ,  $K_{cat1}$  and  $K_{cat2}$  are constants [7,8]. The enzymatic glucose fuel cells use glucose as a fuel to produce electrical energy and enzymes as a biocatalyst to convert chemical energy into electrical energy [2,3]. The anodic reaction is given by the following reaction [9,10] and the cathodic reaction is given by the reaction



Many researchers are interested in the performance of glucose fuel cells. Scott Barton [11] has looked at the

various types of models that can be used to describe enzymatic glucose fuel cells. Debika [12] has attempted to a model batch type direct glucose cells by considering activation, ohmic and concentration over potentials. Rajendran [13] had developed an approximate analytical solution for nonlinear diffusion equations in a mono enzymatic biosensor involving Michaelis Menten kinetics. Malinidevi [14] had developed a model to study the reaction and diffusion of enzymes immobilized in an artificial membrane.

## II. MATHEMATICAL MODEL

The model is assumed as the transport of glucose by diffusion. It is one entity instead of modeling individual components of a cell and one-dimensional transport of hydrogen ion across the fuel cell. The glucose is sent in from the anode to the cathode. The conversion of glucose to hydrogen ion occurs across the enzyme layer that describes a schematic diagram in Figure 3.

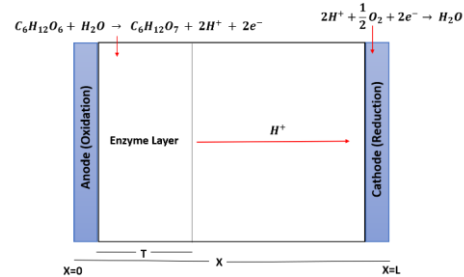


Figure 3: Schematic diagram of an enzymatic glucose fuel cell.

The rate of hydrogen ion can be determined by three reaction rates ( $f(C_G)$ ) are the Michaelis Menten equation, the Morrison equation and the multiple substrate binding sites. Owing to the reaction of enzymatic glucose fuel cells, the transport equation can explain the concentration of glucose ( $C_G$ ) is the following:

$$\frac{\partial C_G}{\partial t} = D_{cG} \frac{\partial^2 C_G}{\partial x^2} - f(C_G), \quad 0 < x < L, t > 0, \quad (6)$$

the initial-boundary conditions are

$$C_G(x, 0) = 1, \quad (7)$$

$$C_G(0, t) = 1,$$

$$\frac{\partial C_G}{\partial x}(L, t) = 0.$$

The hydrogen ion concentration ( $C_{H^+}$ ) satisfies the transport equation for hydrogen ion as the following:

$$\frac{\partial C_{H^+}}{\partial t} = D_{H^+} \frac{\partial^2 C_{H^+}}{\partial x^2} - yD_{H^+} \frac{\partial C_{H^+}}{\partial x} + 2f(C_{H^+}), \quad 0 < x < L, \quad (8)$$

the initial-boundary conditions are

$$\begin{aligned} C_{H^+}(x, 0) &= 0, \\ C_{H^+}(0, t) &= 0, \quad (9) \\ \frac{\partial C_{H^+}}{\partial x}(L, t) &= 0. \end{aligned}$$

Table 1: Positive parameters for the transports of glucose and hydrogen ion concentrations

Symbols	Parameters
$C_G$	Concentration of glucose
$C_{H^+}$	Concentration of hydrogen ion
$D_{cG}$	Diffusion coefficient of glucose
$D_{H^+}$	Diffusion coefficient of hydrogen ion
$[E]$	Enzyme concentration at enzyme layer
$[E_T]$	Total enzyme concentration
$T$	Thickness of the enzyme layer
$K_{cat}$	Kinetic enzyme reaction rate constant for glucose oxidation
$K_m$	Michaelis Menten constant
$\square V$	Dimensional voltage drop across the cell
$\square V^*$	Dimensionless voltage drop across the cell
$L$	Distance between anode and cathode
$y$	Stoichiometric coefficient
$x$	Coordinate direction normal to the anode (m)
$t$	Time (min)

In this paper, the glucose and hydrogen ion concentrations that occur in the enzymatic glucose fuel cells can illustrate as the system of partial differential equations in Eqs.(6)and (8) with three types of reaction rates: the Michaelis Menten equation, the Morrison equation, and the multiple substrate binding sites. We develop symbolic computations in Maple program for computing an equilibrium point, Jacobian matrix and eigen values. Moreover, numerical results for glucose and hydrogen ion concentrations are illustrated by finite difference methods.

**Case 1: The Michaelis Menten equation**

Due to the Michaelis Menten equation in Eq. (1) and the transport equations of glucose concentration ( $C_G = u$ ) and hydrogen concentration ( $C_{H^+} = v$ ) satisfy the system of partial differential equations are given by

$$\begin{aligned} \frac{\partial u}{\partial t} &= D_{cG} \frac{\partial^2 u}{\partial x^2} - \frac{K_{cat}[E]u}{K_m + u}, \quad (10) \\ \frac{\partial v}{\partial t} &= D_{H^+} \frac{\partial^2 v}{\partial x^2} - yD_{H^+} \frac{\square V^*}{L} \frac{\partial v}{\partial x} + 2 \frac{K_{cat}[E]u}{K_m + u}, \end{aligned}$$

Where  $0 < x < L$  and  $t > 0$  with the initial-boundary conditions Eqs. (7),(9). Firstly, we analyze the equilibrium

point( $u^*, v^*$ ) of Eq. (10) by calculating the values of  $u^*, v^*$  in the following system

$$\begin{aligned} -\frac{K_{cat}[E]u^*}{K_m + u^*} &= 0, \\ 2 \frac{K_{cat}[E]u^*}{K_m + u^*} &= 0, \end{aligned}$$

so that, the equilibrium point is  $E_0(u^*, v^*) = (0, v^*)$  when  $v^*$  is any positive. Next, we consider the local stability at  $E_0$  by calculating the Jacobian matrix of Eq. (10) at  $E_0$

$$J_{(0, v^*)} = \begin{bmatrix} -\frac{K_{cat}[E]}{K_m} & 0 \\ 2 \frac{K_{cat}[E]}{K_m} & 0 \end{bmatrix}.$$

The characteristic equation is

$$\begin{aligned} \lambda \left( \frac{K_{cat}[E]}{K_m} + \lambda \right) &= 0, \\ \lambda &= 0, \quad \frac{-K_{cat}[E]}{K_m} \end{aligned}$$

The eigen values are  $\lambda_1 = 0, \lambda_2 = \frac{-K_{cat}[E]}{K_m} < 0$ , thus the

equilibrium point  $E_0$  is locally stable. We use the parameters values in Table 2 to compute the numerical results of glucose and hydrogen ion concentrations with the Michaelis Menten.

Table 2: Value of Parameters (estimation)

Symbols	Parameters	Units
$D_{cG}$	$3.6 \times 10^{-11}$	$m^2 s^{-1}$
$D_{H^+}$	$4.5 \times 10^{-9}$	$m^2 s^{-1}$
$[E]$	$3.645 \times 10^{-7}$	$mol \cdot m^{-2}$
$K_{cat}$	$0.8 \times 10^3$	$s^{-1}$
$K_m$	38	$mol \cdot m^{-3}$
$\square V^*$	0.1	V
$L$	5	m
$y$	2	
$V_{max1}$	0.5	$mol \cdot m^{-2} \cdot s^{-1}$
$V_{max2}$	0.5	$mol \cdot m^{-2} \cdot s^{-1}$
$K_{D1}$	$3.645 \times 10^{-7}$	$mol \cdot m^{-2}$
$K_{D2}$	$7.290 \times 10^{-7}$	$mol \cdot m^{-2}$

The numerical results of the system Eq. (10) with parameter values in Table 2 can be computed by finite difference method. The graphical results of the glucose and

hydrogen ion concentrations with satisfy the initial boundary conditions Eqs. (7),(9) are shown in Figures 4-7.

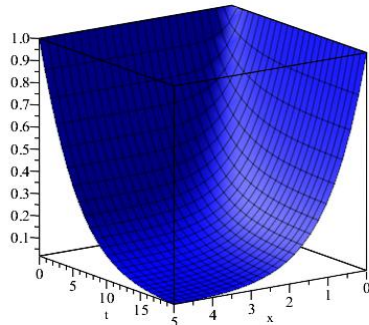


Figure 4: Graph of glucose concentration with the Michaelis Menten equation at  $0 < x < 5, 0 < t < 20$ .

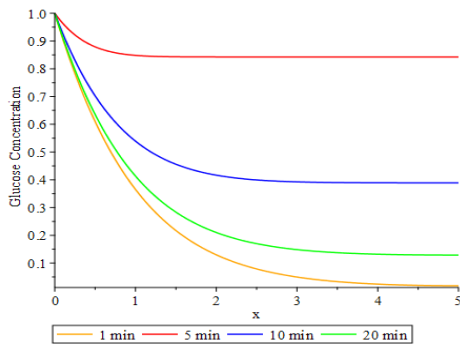


Figure 5: Levels of glucose concentration with the Michaelis Menten equation,  $0 < x < 5, t = 1, 5, 10, 20$ .

Figures 4 and 5, the glucose concentration with the Michaelis Menten decreases along with distance ( $x$ ) and time ( $t$ ). Initially, glucose enters full in the cells (anode), therefore, the domain is held at constant concentration of  $1 \text{ mol} \cdot \text{m}^{-3}$  at  $t = 0$ . Over time the glucose concentration decreases exponential decay with  $t = 1, 5, 10, 20$ , respectively.

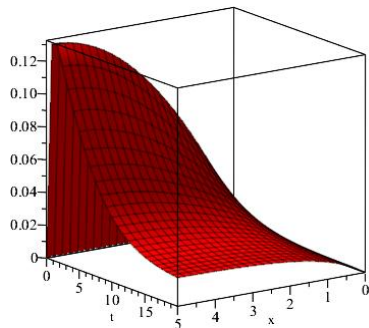


Figure 6: Graph of hydrogen ion concentration with the Michaelis Menten equation at  $0 < x < 5, 0 < t < 20$ .

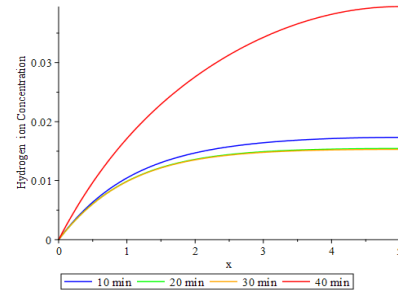


Figure 7: Levels of hydrogen ion concentration with the Michaelis Menten equation  $0 < x < 5, t = 10, 20, 30, 40$ .

Figures 6 and 7 show that the hydrogen ion concentration rapidly increases at the beginning of time ( $t$ ). After that, it slowly increases and tends to the  $v^* > 0$ , which is the equilibrium point.

**Case 2: The Morrison equation (Quadratic velocity equation)**

The second model with the Morrison equation in Eq. (2) of glucose and hydrogen ion concentrations are given by

$$\begin{aligned} \frac{\partial u}{\partial t} &= D_{cG} \frac{\partial^2 u}{\partial x^2} - K_{cat} \frac{(a+u) - \sqrt{(a+u)^2 - 4[E]u}}{2}, \\ \frac{\partial v}{\partial t} &= D_{H^+} \frac{\partial^2 v}{\partial x^2} - yD_{H^+} \frac{V^*}{L} \frac{\partial v}{\partial x} + K_{cat} \left[ (a+u) - \sqrt{(a+u)^2 - 4[E]u} \right], \end{aligned} \quad (11)$$

where  $0 < x < L$ , and  $t > 0$  with the initial-boundary conditions (7),(9). The equilibrium point can be calculated from the system

$$\begin{aligned} -K_{cat} \frac{(a+u^*) - \sqrt{(a+u^*)^2 - 4[E]u^*}}{2} &= 0, \\ K_{cat} \left[ (a+u^*) - \sqrt{(a+u^*)^2 - 4[E]u^*} \right] &= 0. \end{aligned}$$

It's result is the same equilibrium [15] point as the previous model,  $E_1(u^*, v^*) = (0, v^*)$  when  $v^*$  is positive. Calculating the Jacobian matrix of Eq. (11) at  $E_1$  is

$$J_{(0,v^*)} = \begin{bmatrix} -d_1 & 0 \\ 2d_1 & 0 \end{bmatrix},$$

Where,  $d_1 = \frac{K_{cat}[E]}{K_m + [E]}$  which gives  $\lambda(d_1 + \lambda) = 0$ , and eigen values,  $\lambda_1 = 0, \lambda_2 = -d_1 < 0$ , thus the equilibrium point  $E_1$  is local stability.

From Eq. (11), by finite difference method, it obtains the numerical results with including parameter values in

Table 2 and satisfies the initial boundary conditions Eqs.(7),(9)as following in Figures 8-11.

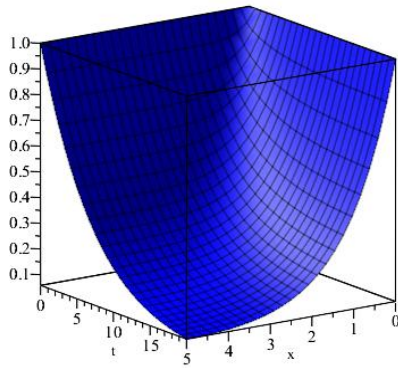


Figure 8: Graph of glucose concentration with the Morrison equation tends to equilibrium point ( $u^* = 0$ ).

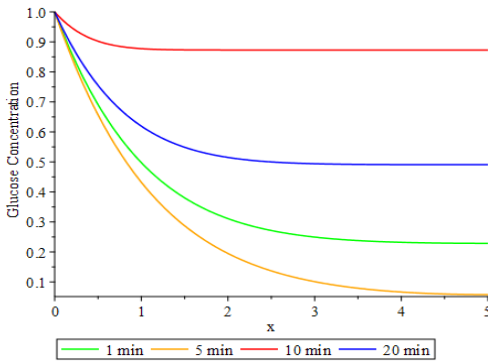


Figure 9: Levels of glucose concentration with the Morrison equation,  $0 < x < 5, t = 1, 5, 10, 20$ .

Figure 9 shows that when  $t = 1, 5, 10, 20$ , the glucose concentration decreases exponential decay entered to steady state ( $u^* = 0$ ).

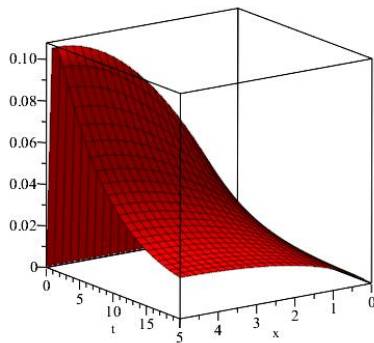


Figure 10: Graph of hydrogen ion concentration with the Morrison equation at  $0 < x < 5, 0 < t < 20$ .

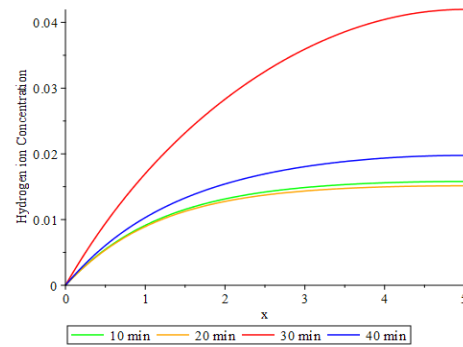


Figure 11 : Levels of hydrogen ion concentration with the Morrison equation,  $0 < x < 5, t = 10, 20, 30, 40$ .

Figures 10 and 11 shows that the hydrogen ion concentration increases across the cells near the cathode ( $x = 5$ ) and slowly increases to the equilibrium point  $v^*, t \rightarrow \infty$ .

### Case 3: The multiple substrate binding sites

The third model with the multiple substrate binding sites in Eq.(3) of glucose and hydrogen ion concentrations are given by

$$\frac{\partial u}{\partial t} = D_{cG} \frac{\partial^2 u}{\partial x^2} - \frac{V_{max1} \frac{u}{K_{D1}} + V_{max2} \frac{u^2}{K_{D1}K_{D2}}}{1 + \frac{u}{K_{D1}} + \frac{u^2}{K_{D1}K_{D2}}}, \quad (12)$$

$$\frac{\partial v}{\partial t} = D_{H^+} \frac{\partial^2 v}{\partial x^2} - yD_{H^+} \frac{\partial v}{\partial x} + 2 \frac{V_{max1} \frac{u}{K_{D1}} + V_{max2} \frac{u^2}{K_{D1}K_{D2}}}{1 + \frac{u}{K_{D1}} + \frac{u^2}{K_{D1}K_{D2}}},$$

where  $0 < x < L$  and  $t > 0$  with the initial-boundary conditions Eqs. (7),(9).The equilibrium point can be calculated from the system

$$\begin{aligned} -\frac{V_{max1} \frac{u^*}{K_{D1}} + V_{max2} \frac{u^{*2}}{K_{D1}K_{D2}}}{1 + \frac{u^*}{K_{D1}} + \frac{u^{*2}}{K_{D1}K_{D2}}} &= 0, \\ 2 \frac{V_{max1} \frac{u^*}{K_{D1}} + V_{max2} \frac{u^{*2}}{K_{D1}K_{D2}}}{1 + \frac{u^*}{K_{D1}} + \frac{u^{*2}}{K_{D1}K_{D2}}} &= 0. \end{aligned}$$

The equilibrium points are  $E_2(u^*, v^*) = (0, v^*)$  and  $E_3(u^*, v^*) = (d_2, v^*)$  when  $d_2 = \frac{-K_{D2}V_{max1}}{V_{max2}} < 0$  and  $v^*$  is positive. As  $d_2$  is negative, we can ignore the equilibrium

$E_3$ . By Analyzing the Jacobian matrix of Eq. (12) at  $E_2$  is computed by

$$J_{(0,v^*)} = \begin{bmatrix} -\frac{V_{max1}}{K_{D1}} & 0 \\ 2\frac{V_{max1}}{K_{D1}} & 0 \end{bmatrix}$$

The characteristic equation is

$$\lambda \left( \frac{V_{max1}}{K_{D1}} + \lambda \right) = 0,$$

$$\lambda = 0, -\frac{V_{max1}}{K_{D1}}.$$

The eigen values are  $\lambda_1 = 0$ ,  $\lambda_2 = -\frac{V_{max1}}{K_{D1}} < 0$ , thus the

equilibrium point  $E_2$  is locally stable. The numerical results using finite difference methods and satisfy the parameter values in Table 2 with the initial boundary conditions Eqs. (7),(9) can be shown as the following Figures 12-15.

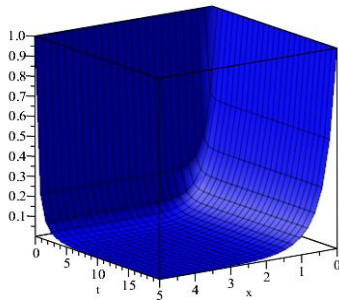


Figure 12: Graph of glucose concentration with the multiple substrate binding sites at  $0 < x < 5$ ,  $0 < t < 20$ .

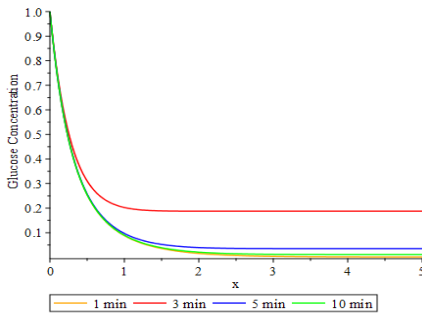


Figure 13: Levels of glucose concentration with the multiple substrate binding sites,  $0 < x < 5$ ,  $t = 1, 3, 5, 10$ .

Figures 12, 13 shows that the glucose concentration when across the cells almost disappear entered to steady state ( $u^* = 0$ ) in the short period.

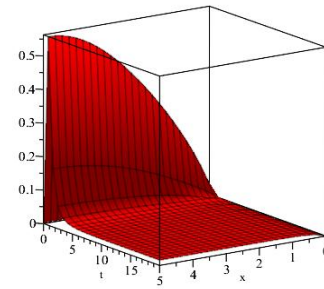


Figure 14: Graph of hydrogen ion concentration with the multiple substrate binding sites at  $0 < x < 5$ ,  $0 < t < 20$ .

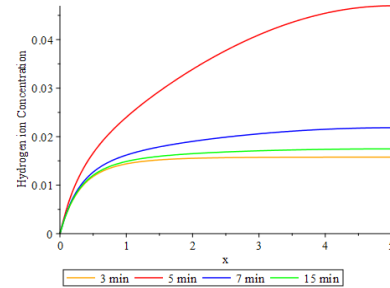
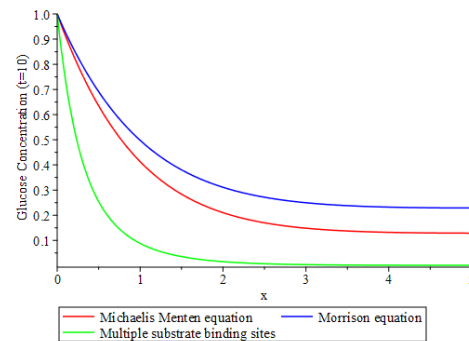


Figure 15: Levels of hydrogen ion concentration with the multiple substrate binding sites,  $0 < x < 5$ ,  $t = 3, 5, 7, 15$ .

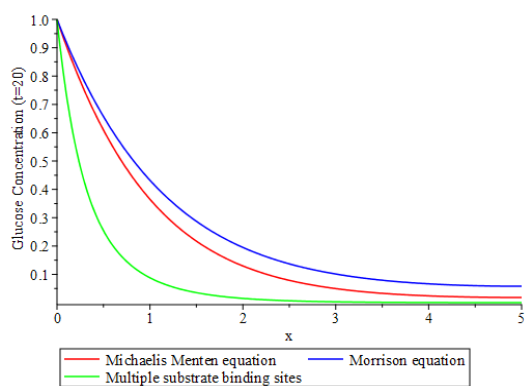
Figures 14, 15 show the hydrogen ion concentration with the multiple substrate binding sites along with the time ( $t$ ) and distance ( $x$ ). It is similar to before two cases of the reaction rate. It approaches the equilibrium point ( $v^* > 0$ ).

### III. COMPARRISON OF NUMERICAL RESULTS

In this section, we compare the glucose and hydrogen ion concentrations with three types of reaction rate for enzyme kinetics: the Michaelis Menten equation, the Morrison equation (Quadratic velocity equation) and the multiple substrate binding sites.



(a)



(b)

Figure 16(a) & (b): Graphs of glucose concentration with three types reaction rates at  $t = 10, 20$ .

Figure 16, the numerical results shows that the multiple substrate binding sites (reaction rate) are the most effective reducing the glucose concentration which approach to zero ( $u^* = 0$ ) in short period. The graphical results show that at  $t = 10$  and  $t = 20$ , the glucose concentration is similarly decreasing, the efficiency of decreasing glucose concentration depends on the multiple substrate binding sites, the Michaelis Menten equation, and the Morrison equation (Quadratic velocity equation), respectively. When  $t$  increases, the glucose concentration decreases faster.

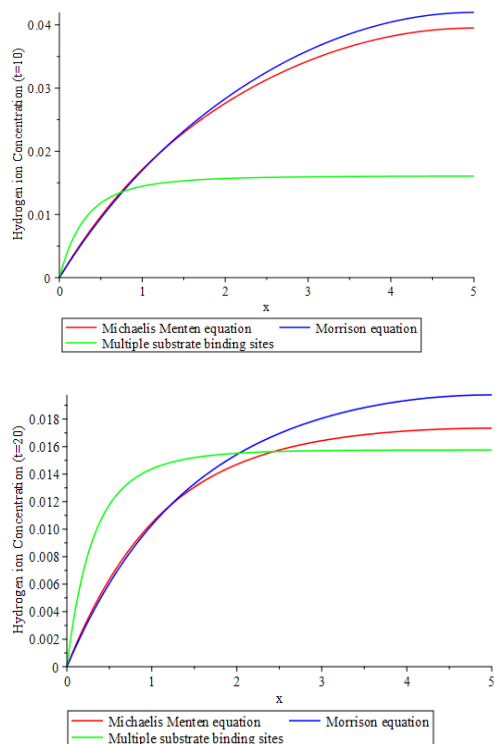


Figure 17: Graphs of hydrogen ion concentration with three types reaction rates at  $t = 10, 20$ .

Figure 17, the most efficient of the reaction rates for increasing the hydrogen ion concentration is the multiple substrate binding sites for a very short period. The reaction rates of the Michaelis Menten equation and the Morrison equation (Quadratic velocity equation) increase at the same level. When time ( $t$ ) getting large, the multiple substrate binding sites are gradually steady, but the Morrison equation (Quadratic velocity equation) and the Michaelis Menten equation still increase eventually.

#### IV. CONCLUSION

The mathematical model is developed to study the enzymatic glucose fuel cells by applying three types of enzyme kinetics including the Michaelis Menten equation, the Morrison equation (Quadratic Velocity Equation) and the multiple substrate binding sites. In numerical results, it is obvious that the glucose concentration decreases across the cells tend to steady-state  $u^* = 0$ . By the reaction rate of the multiple substrate binding sites, it causes the concentration of glucose to rapidly decrease quicker than the Morrison equation and the Michaelis Menten equation, but the hydrogen ion concentration increases. The most efficient reaction rates for increasing the hydrogen ion concentration is the multiple substrate binding sites for a very short period and tend to nonzero steady state.

#### V. ACKNOWLEDGMENT

This work was partially financial supported by the Graduate College and the Department of Mathematics, Faculty of Applied Science, King Mongkut's University of Technology North Bangkok.

#### VI. REFERENCES

- [1] P.Rewatkar, V.P.Hitaishi, E. Lojou, and S. Goel, "Enzymatic fuel cells in a microfluidic environment: Status and opportunities. A mini review," *Electrochemistry Communications*, 2019.
- [2] L. del Torno-de Román, M. Navarro, G. Hughes, J.P. Esquivel, R.D. Milton, S.D. Minter, and N. Sabaté, "Improved performance of a paper-based glucose fuel cell by capillary induced flow," *Electrochimica Acta*, vol. 282, pp. 336-342, 2018.
- [3] V. Z. Rubin, "Current-voltage modeling of the enzymatic glucose fuel cells," *Advances in Chemical Engineering and Science*, vol. 5, no. 02, pp. 164-172, 2015.
- [4] M. A. Burke, "Maini's many contributions to mathematical enzyme kinetics: A review" *Journal of theoretical biology*, vol. 481, pp. 24-27, 2019.
- [5] M. Golićnik, "Evaluation of enzyme kinetic parameters using explicit analytic approximations to the solution of the michaelis-menten equation," *Biochemical Engineering Journal*, vol. 53, no. 2, pp. 234-238, 2011.
- [6] J. Morrison, "Kinetics of the reversible inhibition of enzyme-catalysed reactions by tight-binding inhibitors," *Biochimica et Biophysica Acta(BBA)-Enzymology*, vol. 185, no. 2, pp. 269-286, 1969.
- [7] "Sequential binding." <http://depts.washington.edu/wmatkins/kinetics/sequential.html>. [Last Accessed on: Nov 19, 2019]

- [8] S. Jariwala, S. Phul, R. Nagpal, S. Goel, and B. Krishnamurthy, "Modeling the performance of enzymatic glucose fuel cells," *Journal of Electroanalytical Chemistry*, vol. 801, pp. 354-359, 2017.
- [9] G. Slaughter and T. Kulkarni, "Enzymatic glucose biofuel cell and its application," *Journal of Biochips & Tissue Chips*, vol. 5, no. 1, p. 1, 2015.
- [10] S. Jariwala and B. Krishnamurthy, "Transport equations in an enzymatic glucose fuel cell," *Chemical Physics Letters*, vol. 692, pp. 7-13, 2018.
- [11] S. C. Barton, "1d models for enzymatic biological fuel cells," *The Electrochemical Society Interface*, vol. 24, no. 3, pp. 61-65, 2015.
- [12] D. Basu and S. Basu, "Mathematical modeling of overpotentials of direct glucose alkaline fuel cell and experimental validation," *Journal of Solid State Electrochemistry*, vol. 17, no. 11, pp. 2927-2938, 2013.
- [13] L. Rajendran, M. Kirthiga, and E. Laborda, "Mathematical modeling of nonlinear reaction-diffusion processes in enzymatic biofuel cells," *Current Opinion in Electrochemistry*, vol. 1, no. 1, pp. 121-132, 2017.
- [14] M. Ramanathan, R. Muthuramalingam, and R. Lakshmanan, "The mathematical theory of diffusion and reaction in enzymes immobilized artificial membrane. The theory of the non-steady state," *The Journal of membrane biology*, vol. 248, no. 6, pp. 1127-1135, 2015.
- [15] Teng, Jimmy. "Is Perfect Bayesian Equilibrium a Subset of Nash Equilibrium?." *Journal of Computer Science and Computational Mathematics*, vol. 3, no. 4, 2013.